Atmos. Chem. Phys. Discuss., 9, 12171–12205, 2009
www.atmos-chem-phys-discuss.net/9/12171/2009/

Atmospheric Chemistry and Physics Discussions

This discussion paper is/has been under review for the journal *Atmospheric Chemistry and Physics (ACP)*. Please refer to the corresponding final paper in *ACP* if available.

Satellite NO_2 observations and model simulations of tropospheric columns over South-eastern Europe

I. Zyrichidou[1], M. E. Koukouli[1], D. S. Balis[1], E. Katragkou[1], D. Melas[1], A. Poupkou[1], I. Kioutsioukis[1], R. van der A[2], F. K. Boersma[2], M. van Roozendael[3], and A. Richter[4]

[1]Laboratory of Atmospheric Physics, Physics Department, Aristotle University of Thessaloniki, Thessaloniki, Greece
[2]Royal Netherlands Meteorological Service, De Bilt, The Netherlands
[3]Belgian Institute for Space Aeronomy, Brussels, Belgium
[4]Institute of Environmental Physics, University of Bremen, Germany

Received: 6 April 2009 – Accepted: 10 May 2009 – Published: 19 May 2009

Correspondence to: D. S. Balis (balis@auth.gr)

Published by Copernicus Publications on behalf of the European Geosciences Union.

Abstract

Satellite observations of nitrogen dioxide (NO_2) tropospheric columns over Southeastern Europe are analyzed to study the characteristics of the spatial and temporal variability of pollution in the area. The interannual variability of the tropospheric NO_2 columns is presented over urban, rural and industrial locations based on measurements from four satellite instruments, GOME/ERS-2, SCIAMACHY/Envisat, OMI/Aura and GOME-2/MetOp spanning a period of over twelve years. The consistency between the different datasets over the area is investigated. Two operational algorithms for the retrieval of tropospheric NO_2 are considered, the one developed jointly by the Royal Netherlands Meteorological Institute and Belgian Institute for Space Astronomy and the one developed by the University of Bremen. The tropospheric NO_2 columns for the area under study have been simulated for the period 1996–2001 with the Comprehensive Air Quality Model (CAMx) and are compared with GOME measurements. Over urban and industrial locations the mean tropospheric NO_2 columns range between 3 and 7.0×10^{15} molecules/cm^2, showing a seasonal variability with a peak to peak amplitude of about 6.0×10^{15} molecules/cm^2, while the background values over rural sites are close to 1.1×10^{15} molecules/cm^2. Differences in the overpass time and spatial resolution of the different satellites, as well as differences in the algorithms, introduce significant differences in the estimated columns however the correlation between the different estimates is higher than 0.8. It is found that the model simulations reveal similar spatial patterns as the GOME observations, a result which is consistent with both algorithms. Although the model simulations show a mean bias of −0.1 under clean conditions, the modeled temporal correlation of 0.5 is poor in absence of biogenic and biomass burning emissions.

ACPD

9, 12171–12205, 2009

1 Introduction

Nitrogen dioxide plays a key role in tropospheric chemistry with important implications for air quality and climate change. Measurements of nitrogen dioxide (NO_2) are important for the understanding of tropospheric and stratospheric chemistry, particularly in relation to ozone production and loss (e.g. Crutzen, 1979). On the one hand, tropospheric NO_2 is essential for maintaining the oxidizing capacity of the atmosphere. Photolysis of NO_2 during daytime is the major source of ozone (O_3) in the troposphere and photolysis of O_3 in turn initializes the production of the hydroxyl radical (OH), the main cleansing agent of the atmosphere. On the other hand, NO_2 as well as O_3 are toxic to the biosphere and may cause respiratory problems for humans. Moreover, NO_2 may react with OH to form nitric acid (HNO_3), one of the main components of acid rain. As a greenhouse gas, NO_2 contributes significantly to radiative forcing over industrial regions, especially in urban areas (e.g. Solomon et al., 1999), due to its short lifetime, and hence has a local and not global effect. Although the direct contribution of tropospheric NO_2 to global warming is relatively small, emissions of nitrogen oxides ($NO_x \equiv NO+NO_2$) affect the global climate indirectly by perturbing O_3 and methane (CH_4) concentrations. More details on the chemistry of tropospheric NO_2 are given, for example, by Seinfeld and Pandis (1998) and Finlayson-Pitts and Pitts (2000). The abundance of NO_2 in the troposphere is highly variable and influenced by both anthropogenic and natural emissions (e.g. Bradshaw et al., 2000). On a global scale, the main sources of nitrogen oxides are fossil fuel combustion, biomass burning, lightning and microbiological processes in soil (e.g. Lee et al., 1997).

In the past, NO_2 fluxes could be assessed by modeling, aircraft and ground-based measurements or using a combination of the above (Dickerson, 1984; Lelieveld et al., 1989; Lefohn and Shadwick, 1991). However, following the advances in satellite technology and the development of new instruments and algorithms the observation of NO_2 columns from space has become a reality. A global picture of the spatial distribution of tropospheric NO_2 is now obtainable since satellite measurements provide a global

ACPD
9, 12171–12205, 2009

coverage in a very short time (between 1 and 6 days depending on instrument and cloud cover).

Tropospheric NO_2 columns retrieved from the Global Ozone Monitoring Experiment (GOME), the Scanning Imaging Absorption spectroMeter for Atmospheric CartograpHY (SCIAMACHY) and the Ozone Monitoring Instrument (OMI) span more than ten years and have been used for air quality studies and satellite instrument validations (Richter et al., 2000, 2005; van der A et al., 2006, 2008). Most of these studies focus on Asia, as this part of the planet currently shows the largest variability and increasing trends in species relevant for air quality. As was shown in van der A et al. (2008) there is an interesting outflow of anthropogenic NO_2 over the oceans at the East coast of North America and China. A large positive trend is clearly visible in East China as has been reported in Richter et al. (2005) where it is shown that a strong increase in NO_x emissions in China due to an increase in industry and traffic has been detected from 1996 to 2005 using a combination of GOME and SCIAMACHY observations. A yearly growth was determined in terms of percentage with respect to the initial NO_2 concentrations from 1996 which was 10±4% over Beijing, 2.2±2% over Sao Paulo and 1.7±1% over Mexico City (van der A et al., 2006). There are also clear spots of increasing NO_2 in Mid-USA, South Africa, Delhi (India), Tehran (Iran) and surrounding areas, and several cities in mid-Russia. Furthermore, outflow of biomass burning NO_2 is visible west of Africa and Australia (van der A et al., 2008).

Many studies have also recently used tropospheric NO_2 satellite measurements in order to validate air quality models. In van Noije et al. (2006) different NO_2 retrievals have been inter-compared and also compared with results from 17 atmospheric chemistry models on a global scale. They found that on average the models underestimate the retrievals in industrial regions and overestimate the retrievals in regions dominated by biomass burning. In Uno et al. (2007) systematic analyses of inter-annual and seasonal variability of tropospheric NO_2 vertical column densities based on GOME satellite observations and the regional scale CTM CMAQ (Community Multi-scale Air Quality) were presented over Asia. CMAQ results underestimated GOME retrievals by factors

of 2–4 over polluted industrial regions.

To date no clear assessment of the behavior of nitrogen dioxide over the Balkan Peninsula exists. Few studies have localized their results over this part of Europe. For instance, in Ladstätter-Weiβenmayer et al. (2007) the synergistic use of GOME tropospheric column data (version 1, developed at the University of Bremen) with back-trajectory analysis and box model calculations enabled the detection of significant changes in pollutant tropospheric columns related to general air circulation patterns. It was found that when the Mediterranean is influenced by air masses from Central Europe, the Balkans and the Black Sea, pollution leads to an increase in NO_2. Furthermore, the observed mean NO_2 tropospheric column densities (in 10^{15} molecules/cm^2) were determined to be: for Crete 1.1, for Athens 2.0, for Thessaloniki 2.3 and for Istanbul 2.4 for the month of May as a mean value of the years 1996 to 2002. A detailed analysis for Western Europe was presented by Blond et al. (2007), who compared tropospheric NO_2, from a vertically extended version (up to 200 hPa) of CHIMERE with high-resolution column observations from SCIAMACHY as retrieved by BIRA/KNMI. Konovalov et al. (2005) used GOME-based data products (version 2, developed at the University of Bremen), to evaluate the CHIMERE CTM over Western (10° W, 186° E, 35° N and 60° N) and Eastern (18° E, 65° E, 40° N and 65° N) Europe. Their study indicated much lower levels of NO_2 in Eastern Europe (which includes the Balkan Peninsula) compared to Western Europe and no clear evidence could be found that either the performance of CHIMERE or the quality of NO_2 columns derived from GOME measurements performs poorer for Eastern than for Western Europe.

The Eastern Mediterranean is a known cross road of air masses where anthropogenic pollution emissions converge with natural ones (e.g. Lelieveld et al., 2002, Mihalopoulos, 2007). Since the presently available ground-based stations do not have a proper spatial distribution in South Eastern Europe (Mihalopoulos, 2007) and there are not many scientific studies that focus on NO_2 variability over the Balkan Peninsula, the present study aims at providing more details on the temporal and spatial distribution of tropospheric NO_2 columns over the area through satellite observations and

model simulations and to examine the satellites' consistency over areas with moderate loading of tropospheric NO_2.

In Sect. 2 we give a description of the instruments, the algorithms and the photochemical model we used in our analysis. In Sect 3 we investigate the long-term variability of tropospheric NO_2 over several Balkan geolocations as derived from GOME, SCIAMACHY, OMI and GOME-2 retrievals in order to assess the ability of satellite sensors to detect pollution and to investigate if significant trends can be derived on a regional scale. In addition, we compare concurrent (on the same day and on the same geolocation) satellite measurements. This comparison is used to infer whether or not the satellite data are consistent over the region under study. In the last part of Sect. 3 we evaluate the CAMx model using satellite retrievals from both the KNMI/BIRA and the Institute of Environmental Physics (IUP), University of Bremen DOAS algorithms. Finally, in Sect. 4 we present the conclusions derived from this study.

2 Methodology and data

Thirty-two geolocations around the Balkan Peninsula were chosen as focal point for this study (Fig. 1) and are listed in Table 2. They were selected according to the following criteria: their spatial distribution around the region, polluted cities such as industrial and commercial centers or capitals, unpolluted cities that can provide background values and cites that may help the detection of potential transboundary transport of NO_2 inside the Balkan Peninsula. For all these locations overpass files for the tropospheric NO_2 columns were generated from level-2 data of GOME, SCIAMACHY, OMI and GOME-2. The extraction criteria and the main characteristics of the instruments and the algorithms are discussed in the following paragraphs of this section.

ACPD
9, 12171–12205, 2009

2.1 Instruments

The GOME instrument is a nadir-viewing spectrometer that measures upwelling radiance from the atmosphere and solar irradiance, covering the spectral range of 240 nm to 790 nm at a spectral resolution of 0.2–0.4 nm. Global coverage is achieved within three days at the equator and within one day at 65° latitude. The GOME instrument principles are described by Burrows et al., 1999.

SCIAMACHY is a passive remote sensing spectrometer observing backscattered, reflected, transmitted and emitted radiation from the atmosphere and the Earth's surface, in the wavelength range between 240 nm and 2380 nm and with a spectral resolution of 0.25 nm in the UV and 0.4 nm in the visible. SCIAMACHY alternately makes limb and nadir measurements. Global coverage at the equator is achieved in six days and more frequently at higher latitudes. The SCIAMACHY measurement principles are described in Bovensmann et al., 1999.

The Dutch – Finnish OMI is the first of a new generation of space borne spectrometers that combine a high spatial resolution with daily global coverage because of the wide swath of the measurement. OMI is a nadir viewing imaging spectrograph measuring direct and backscattered sunlight in the ultraviolet – visible (UV/VIS) range from 270 nm to 500 nm with a spectral resolution of about 0.5 nm and is described in detail in Levelt et al., 2006.

The GOME-2, an improved version of ESA's GOME instrument, is a nadir – looking UV – visible spectrometer. GOME-2 covers the spectral range between 240 nm and 790 nm and has a spectral resolution between 0.25 nm and 0.5 nm and provides global coverage within 1.5 days. The GOME-2 instrument principles are described in Callies et al. (2000).

The main features of the four instruments, satellite platforms and data versions used in this study are summarized in Table 1 for quick reference.

ACPD
9, 12171–12205, 2009

2.2 GOME, SCIAMACHY, OMI and GOME-2 tropospheric NO_2 retrievals

The main data set used in this study are NO_2 vertical tropospheric column densities retrieved by KNMI (Royal Netherlands Meteorological Institute) and BIRA/IASB (Belgian Institute for Space Astronomy) which are publicly available on a day-by-day basis via ESA's TEMIS project (http://www.temis.nl). In this study we also considered GOME NO_2 data from IUP Bremen which are available via http://www.iup.uni-bremen.de. This paper however does not aim to provide a detailed intercomparison between the two algorithms and the two satellite data sets. The two algorithms are independently compared with model simulations for the period when GOME measurements are available. They are referred to as GOMEtemis for the KNMI/BIRA algorithm and GOMEbremen for the IUP Bremen algorithm. Also, OMI measurements are referred to as OMIT3 in plots.

2.2.1 KNMI/BIRA algorithm

The TEMIS NO_2 vertical tropospheric column for GOME, SCIAMACHY and GOME-2 tropospheric NO_2 columns are all products of the same retrieval algorithm. The retrieval of tropospheric NO_2 is performed in three steps: first the total slant NO_2 column density is retrieved by BIRA/IASB using a Differential Optical Absorption Spectroscopy (DOAS) technique (e.g. Platt, 1994), then the stratospheric contribution is deduced by assimilating the total slant column data in the TM 4 chemistry model driven by meteorological analysis from the European Center for Medium-range Weather Forecasts (ECMWF) and subsequently the vertical tropospheric column is derived, applying a tropospheric air mass factor correction. More details on the retrieval can be found in Boersma et al. (2004) and in Blond et al. (2007). The KNMI/BIRA tropospheric NO_2 retrievals have been also validated in several studies (e.g. Schaub et al., 2006; Blond et al., 2007; Lambert et al., 2007)

The OMI retrievals were developed at KNMI within the DOMINO (Dutch OMI NO_2) project. The DOMINO product is available from www.temis.nl. The DOMINO retrieval

algorithm is described elaborately in Boersma et al., 2007 and recent updates can be found in the DOMINO Product Specification Document (http://www.temis.nl/docs/OMI_NO2_HE5_1.0.2.pdf). The DOMINO tropospheric NO_2 columns have been validated versus independent measurements during various campaigns (Boersma et al., 2008a, 2009).

For the purpose of our study we note that the cloud fraction for GOME, SCIAMACHY and GOME-2 is taken from the Fast Retrieval Scheme for Clouds from the oxygen A band (FRESCO) algorithm (Koelemeijer et al., 2001). OMI's cloud fraction is provided by a cloud retrieval algorithm that uses the absorption of the O_2-O_2 collision complex near 477 nm (Acarreta et al., 2004). The FRESCO and O_2-O_2 algorithms are based on the same set of assumptions, i.e. they both retrieve an effective cloud fraction (clouds are modeled as Lambertian reflectors) that holds for a cloud albedo of 0.8. (Boersma et al., 2007).The similarities and the significant differences between the cloud parameter retrievals from SCIAMACHY and OMI are described quite extensively in Boersma et al., 2007. In that paper, since temporal variation in global cloud fraction and cloud pressure between 10:00 and 13:45 local time is small (Bergman and Salby, 1996), an evaluation of the consistency between the two cloud parameters was made as well. The comparison of the FRESCO and O_2-O_2 cloud algorithms showed that on average SCIAMACHY cloud fractions are higher by 0.011 than OMI cloud fractions and OMI cloud pressures are about 60 hPa higher than FRESCO cloud pressures (for cloud fractions >0.05).

For our spatial and temporal variability analysis only observations with a radiance reflectance of less than 50% from clouds were used which corresponds to a cloud fraction of less than about 20% (van der A et al., 2008). In addition, only completely unflagged retrievals were accepted. For all the satellite instruments the distance between the satellite's center field of view and the ground locus was set to 50 km, in order to obtain spatially comparable measurements. This distance was the minimum we could choose to use in our analysis so as to get adequate or coincident measurements from each satellite for the intercomparisons. Finally, we used only the forward scans

ACPD
9, 12171–12205, 2009

for GOME, SCIAMACHY, and GOME-2 and from OMI pixels with CTP (Cross Track Position) 10 to 50.

2.2.2 BREMEN algorithm

As mentioned above, apart from the KNMI/BIRA product, in this paper we also use the GOME tropospheric NO_2 columns from the Institute of Environmental Physics of the University of Bremen. The GOME tropospheric NO_2 retrieval method is performed in a series of similar steps as those described above: the total NO_2 slant column is extracted using the DOAS method, the stratospheric contribution is subtracted and then, via an air mass factor calculation, the remaining tropospheric NO_2 slant column is converted to a geometry independent tropospheric NO_2 vertical column. The retrieval algorithm is described in details in Richter and Burrows, 2002 and Richter et al., 2005.

The differences, and similarities, of the two algorithms are mentioned briefly below:

1. The *DOAS method* is applied for the 405–465 nm region for OMI and for the 420–450 nm region for SCIAMACHY and GOME(-2) in the KNMI/BIRA algorithm and for the 425–450 nm region for GOME in the IUP/Bremen technique.

2. KNMI/BIRA has developed an assimilation approach in which the GOME slant columns force the *stratospheric component* of NO_2 of the Tracer Model Version 4 (TM4) to be consistent with the observations (Boersma et al., 2004). In IUP/Bremen stratospheric NO_2 fields from the SLIMCAT model are used (Chipperfield et al., 1999), scaled such that they are consistent with the GOME observations in the Pacific Ocean reference sector (Savage et al., 2004; Richter et al., 2005).

3. For the *air mass factor* calculation BIRA/KNMI use the Doubling Adding KNMI (DAK) code (de Haan et al., 1987; Stammes et al., 1989) and IUP/Bremen use the SCIATRAN algorithm (Rozanov et al., 1997).

4. Both KNMI/BIRA and IUP/Bremen use *cloud fraction and cloud top height* from the Fast Retrieval Scheme for Cloud Observables (FRESCO) (Koelemeijer et al., 2001) which treats clouds as Lambertian surfaces for the GOME retrievals. For the KNMI/BIRA retrieval the influence of small cloud fractions is explicitly accounted for whereas IUP/Bremen discards measurements with a cloud fraction of more than 0.2 and does not apply any correction for residual clouds.

5. The *surface albedo* for the BIRA/KNMI retrieval is based on TOMS albedos (a combination of Herman and Celarier, 1997 and Koelemeijer et al., 2003 as described in Boersma et al., 2004) which are wavelength corrected with the ratio of GOME reflectivities at 380 nm and 440 nm, whereas the IUP/Bremen retrievals are based on the GOME surface reflectivities (Koelemeijer et al., 2003).

6. In the air mass factor calculation, the *NO_2 profile shape* is extracted from collocated daily profiles at the appropriate overpass time from the Tracer Model Version 4 (TM4) model for KNMI/BIRA whereas IUP/Bremen use monthly averages from a global CTM model, MOZART, version 2 output for the year 1997 (Horowitz et al., 2003).

7. The BIRA/KNMI algorithm does not explicitly account for *aerosol* effects, assuming that they are at least partially accounted for by the cloud retrieval algorithm, whereas the IUP/Bremen retrieval accounts for three different aerosol scenarios (maritime, rural, and urban) taken from the Low Resolution Transmission (LOWTRAN) database.

Almost eight years of continuous tropospheric NO_2 measurements from GOME/ERS-2 from the IUP/Bremen algorithm are used in this paper. The same extraction criteria as for the KNMI/BIRA retrievals have been used.

ACPD
9, 12171–12205, 2009

2.3 CAMx model

The **C**omprehensive **A**ir Quality **M**odel with e **x**tensions (CAMx) version 4.40 is a publicly available open-source computer modeling system for the integrated assessment of gaseous and particulate air pollution (www.camx.com). The CAMx simulation presented in this study is based on run with coarse grid spacing over Europe in a spatial resolution of 50×50 km, identical to the grid defined for the meteorological runs. The domain's vertical profile contains 12 layers of varying thickness, extending up to 450 hPa. The meteorological fields were derived from REGional Climate Model (RegCM3, http://www.ictp.trieste.it/ ~pubregcm/RegCM3) runs which were forced by the ERA-40 reanalysis fields (2.5°×2.5°, L23 pressure levels) of the European Centre for Medium-Range Weather Forecasts (ECMWF). Data for the calculation of hourly anthropogenic emissions were extracted from the European Monitoring and Evaluation Programme EMEP database (http://www.emep.int/) while organic biogenic emissions were calculated on-line using the RegCM-CAMx interface on a 6-hourly basis. Emissions from lightning and biomass burning activities were not considered in the model runs. The boundary conditions were set to 1 ppb. A more detailed description of the modeling system can be found in Katragkou et al., 2009.

NO_2 tropospheric vertical column densities were extracted for the altitudes between 0–7 km and the time period from 01/01/1996 to 31/12/2001 for which the model run has been performed. We compared average 2-hour NO_2 predictions from CAMx with the GOME measurements, using an appropriate number of CAMx grid-cells in a way that they fit in with GOME's pixel spatial resolution.

3 Results and discussion

3.1 Temporal variability

For all the locations listed in Table 2 we compiled time series of the monthly mean tropospheric NO_2 columns for each satellite instrument and algorithm using the criteria mentioned in the previous section, in order to examine to what extend we can determine certain characteristics of the temporal variability of tropospheric NO_2 over urban, rural and industrial areas in the region. In this paragraph we present representative examples of time series of the monthly mean tropospheric NO_2 column densities for an urban, an industrial and a rural region in order to investigate the mean levels and the seasonal evolution of the observations from the four satellites. These time series are shown in Fig. 2 for Thessaloniki (urban), Maritsa (industrial) and Finokalia (rural). The satellite algorithm results shown in this figure and further on, unless stated otherwise, are the KNMI/BIRA algorithm retrievals.

Figure 2 demonstrates that SCIAMACHY, GOME-2 and OMI can reveal the characteristics of urban scale and industrial regions due to their finer horizontal resolutions and are quite consistent, while GOME is representative of a much larger area which smoothes out the effect of these local sources. Over the polluted sites there is a relative offset between SCIAMACHY and OMI measurements as shown here, as typical examples, for Maritsa (upper right) and Thessaloniki (upper left). The estimated average values for Thessaloniki and Maritsa are $3.8\pm1.7\times10^{15}$ molecules/cm^2 and $3.2\pm1.0\times10^{15}$ molecules/cm^2 respectively as derived from OMI monthly mean measurements, while the corresponding values estimated from SCIAMACHY are $4.0\pm2.36\times10^{15}$ molecules/cm^2 and $2.7\pm0.9\times10^{15}$ molecules/cm^2. This discrepancy between SCIAMACHY and OMI can be possibly attributed to the different local crossing time of each satellite, (around three hours difference), and to the fact that the local NO_2 diurnal variability may quite possibly be different for each location. This offset is discussed in more detail in Sect. 3.2. Both over urban and industrial regions OMI and SCIAMACHY measurements show a seasonal variability with maximum values during

ACPD
9, 12171–12205, 2009

the winter months and minimum values during summer. The peak-to-peak amplitude of this variability over urban and industrial regions is consistent, and ranges from 4.0 to 6.0×10^{15} molecules/cm^2. The collocation criteria used (see Sects. 2.2 and 2.3) do not provide a continuous time series for GOME due to its orbit and pixel characteristics. However indications for the seasonal variability, consistent with SCIAMACHY and OMI, are also observed in GOME data. Without extensively homogenizing the four different data sources and the subsequent loss of spatial resolution, an analysis which is beyond the scope of this paper, possible trends over the region in question cannot be extracted in a statistical significant way. Even over rural areas such as Finokalia, the differences in overpass time and spatial resolution are sufficient to preclude a statistically significant result. In Fig. 2 the case of Istanbul is also presented as it is the most polluted region examined in this work. Over the largest city of Turkey, the highest values of tropospheric NO_2 were observed for the entire period considered and a mean value of $7.9\pm3.2\times10^{15}$ molecules/cm^2 as derived from OMI observations is found with a seasonal variability similar to the other urban sites examined. Onkal-Engin et al., 2004 have shown that these levels of pollution are mainly due to emissions of intense land transportation in Istanbul.

In a rural area like Finokalia, with no large sources of NO_2 in the surroundings, the mean tropospheric NO_2 amounts are close to 1.0×10^{15} molecules/cm^2 and they show a small seasonal variability with an amplitude around 0.5×10^{15} molecules/cm^2 with higher values observed during summer. There are no significant discrepancies among the different satellite instruments. In addition when combining the time series from the different satellites (GOME-SCIAMACHY-OMI) there is no sign for a long-term change in tropospheric NO_2 columns over the rural areas studied here, indicating almost constant background conditions in the greater area.

The discrepancies between the different satellite products shown in the analysis discussed in this section are investigated further in the following section.

3.2 Satellite intercomparison

In this section, different satellite products are inter-compared using SCIAMACHY measurements as reference, as they provide a concurrent dataset with the other three instruments. Figure 3 compares monthly mean tropospheric NO_2 derived from the four satellites for all geolocations at the same dates. The comparison between GOME and SCIAMACHY which have a common dataset of 12 months show very good agreement with a correlation coefficient of 0.9 mainly due to their similar overpass times. The correlation coefficient between OMI and SCIAMACHY is 0.86. The differences between OMI and SCIAMACHY are mainly credited to different overpass times and can be attributed to a moderate diurnal cycle in emissions (see Fig. 4, left panel) in combination with a strong diurnal cycle in photochemistry with maximum NO_2 loss around noon. A larger scatter between the OMI and SCIAMACHY data (middle plot) should also be expected due to their different horizontal resolution. OMI is expected to detect higher NO_2 values from more localized sources, for e.g. industries, biomass burning, and soil emissions. SCIAMACHY and GOME-2 measurements (bottom plot) are also well correlated due to their similar overpass times and horizontal coverage and so their spatial distributions have a correlation coefficient r of 0.85. For tropospheric columns less than 4.0×10^{15} molecules/cm^2 we conclude that SCIAMACHY is in good agreement with GOME, OMI and GOME-2. For tropospheric columns larger than 4.0×10^{15} molecules/cm^2 there are more discrepancies between the satellite measurements.

In order to investigate the systematic differences between SCIAMACHY and OMI, we used the CAMx model predictions to examine if the 13:30 to 10:00 UT differences in tropospheric NO_2 columns observed by satellites in this region are consistent with the diurnal variations predicted by a photochemical model. The left plot of Fig. 4 depicts the mean diurnal variation of tropospheric NO_2 columns (solid line) for the entire domain area as simulated by the model and coincident and averaged measurements for the years 2004–2007 by SCIAMACHY and OMI. In Fig. 4 (left plot) it is apparent

ACPD
9, 12171–12205, 2009

that CAMx NO_2 columns increase in the late afternoon, reflecting the diurnal cycle of NO_2 emissions considered in the model (see crosses in left panel of Fig. 4), that have a broad daytime maximum. The most geolocations used in this study are urban and so CAMx emissions show a daytime maximum that mainly reflects intense vehicle use in the early morning and mostly in the late afternoon. The satellite results show that the mean NO_2 columns observed from OMI are 3.03% smaller than those shown by SCIAMACHY, and this finding is consistent with the expected average diurnal variability estimated by the model simulations (1.58 %). This relative 13:30 to 10:00 UT ratio decrease is consistent with Boersma et al. (2008b) who found that there is a relative decrease in NO_2 column from 10:00 to 13:30 (6% for the satellite observations and 13% for the GEOS-Chem simulations for Europe and even larger for Northeastern United States and China). This decrease can be explained by the broad daytime maximum of the emissions and the stronger photochemical loss in the hours before the OMI overpass compared to the hours before the SCIAMACHY overpass (Boersma et al., 2008b). The chemical loss of NO_x to HNO_3 (through the gas phase NO_2+OH reaction and by hydrolysis of N_2O_5 in aerosols) occurs throughout the diurnal cycle but is strongest at midday, when OH concentrations are highest. The 13:30/10:00 LT ratio is not constant throughout the year and the relative difference of OMI estimates versus SCIAMACHY shows a clear seasonal behavior. This seasonality is demonstrated in the right panel of Fig. 4 where we present the seasonal variability of the ratio of tropospheric NO_2 columns from 10:00 LT to 13:30 LT (OMI vs SCIAMACHY) and 10:00 LT to 14:00 LT (CAMx model). The satellite measurements used here are concurrent in order to avoid introducing a sampling bias. As we can see from the satellite measurements and model simulations the observed and predicted 13:30/10:00 LT ratio of tropospheric NO_2 both show a consistent seasonality only for the winter months (December–April). The 13:30 to 10:00 ratios smaller than one are on average larger between February and April and smaller between January and May. During the summer months (May–October) there is a discrepancy in the seasonality between measurements–based and simulation-based ratios, i.e. OMI data of the same day are higher than SCIAMACHY

data for the summer months, which is not reproduced by the model. Similar behavior has been also observed by Boersma et al., 2008b for areas with large biomass burning events. The emissions in the model do not consider biomass burning, which, according to fire spots available in the World Fire Atlas (http://wfaa-dat.esrin.esa.int/), has a maximum during the warm season (Fig. 4 right panel). This discrepancy was indeed larger for years with intense fire activity in and around the area (2005 and 2007) relative to a year with moderate fire activity (2006). Since biomass burning emissions are not included in CAMx, this inversion of the ratio cannot be verified by the model and will be examined in a future study.

3.3 Evaluation of CAMx for the time period 1996–2001

In this section we investigate the consistency of the spatial and temporal variability of NO_2 tropospheric columns measured by GOME and predicted by CAMx. Although GOMEtemis and GOME Bremen look very similar at first sight our analysis, involving the CAMx model, reveals subtle differences.

Figure 5 presents scatter plots of the monthly tropospheric NO_2 columns from the Bremen (left) and KNMI/BIRA (right) algorithms for concurrent measurements and CAMx predictions. The correlation between both GOME algorithm measurements and CAMx predictions is not very high ($R \approx 0.5$). As discussed earlier this is probably due to missing CAMx emissions (biomass burning), to CAMx background conditions (no long range transport is considered from sources outside the modeling domain) and also to the fact that the model resolution is 50×50 km, much finer than GOME's. GOME-Bremen data show a better correlation (0.7) especially below 0.3 molecules/cm^2 (Boersma et al., 2004) results in a slightly different number of observations between the two data sets. The root mean square error (RMSE) between CAMx and GOME data is less than 2.0×10^{15} molecules/cm^2 in all cases and the mean bias (MB) is less than 0.2×10^{15} molecules/cm^2 when considering GOME-TEMIS data and less than 0.5×10^{15} molecules/cm^2 when considering GOME-Bremen data. These results are consistent with the result shown in the TEMIS Algorithm Document for Tro-

pospheric NO_2 where the tropospheric NO_2 columns from SCIAMACHY are compared to outputs from the CHIMERE model, as shown in Table 3. The normalized mean bias (NMB), considering the monthly mean values, is −4.02%, 3.65% and −8%, whereas considering the Bremen algorithm is 30.27%, 5.36% and −1.19% over industrial, rural and urban regions respectively.

Figure 6 shows the scatter between GOME monthly mean tropospheric NO_2 columns for 1996–2001 from both algorithm retrievals for all geolocations (only values greater than 0.3×10^{15} molecules/cm^2 (Boersma et al., 2004) were used). The spatial distributions of the two GOME retrievals have a correlation coefficient R=0.81, that points to the high consistency of the two algorithms. GOMEtemis results slightly overestimate GOMEbremen results over the urban and industrial areas, whereas the agreement is much better over rural regions with low tropospheric NO_2 values.

The comparison between the average columns of predicted (CAMx) and observed (GOMEtemis) mean tropospheric NO_2 columns for thirty one of the chosen geolocations for the years 1996–2001 can be seen in Fig. 7 (left).Each diamond symbol corresponds to the average tropospheric NO_2 column, derived from concurrent daily values for the time period 1996–2001, over a geolocation. There is quite good correlation between the measurements and the modeling predictions, with CAMx slightly underestimating the mean GOMEtemis observations by around 1.0×10^{15} molecules/cm^2 over the most polluted regions because model initial and boundary (top and lateral) conditions corresponds to concentrations of clean air. In Fig. 7 (right) GOMEbremen data are also well correlated with CAMx simulations (correlation coefficient equals to 0.72). In both cases CAMx overestimates GOME measurements by around 0.5×10^{15} molecules/cm^2 mostly over rural areas and regions where model background emissions are not well-determined. The Istanbul mean value is excluded from these plots because the emission inventory used (EMEP based) provided unrealistically low estimates for the city and it was considered not representative for this area.

4 Summary and conclusions

We have intercompared satellite retrievals of tropospheric NO_2 columns from four different instruments, namely GOME/ERS-2, SCIAMACHY/Envisat, OMI/Aura and GOME-2/MetOp, using similar retrieval methods for a time period of more than ten years and we have examined the temporal variability of tropospheric NO_2 vertical columns over Balkan regions deduced by KNMI/BIRA satellite retrievals. We have further evaluated modeling (CAMx) simulations by comparing them with GOME observations from two different algorithms (KNMI/BIRA and IUP Bremen). The main findings of this work may be summarized as follows:

The maximum mean value of tropospheric NO_2 over the Balkan region, as derived from the satellite measurements, is observed over Istanbul, with values of 6.0±4.5, 8.4±7.0, 6.5±6.1 and 7.1±6.0×10^{15} molecules/cm^2 from GOME, SCIAMACHY, OMI and GOME-2 respectively. Over other large urban areas the mean NO_2 tropospheric column densities range, depending on the observing satellite, between 3.0 and 5.0×10^{15} molecules/cm^2 with indications for a seasonal variability with and amplitude of 6.0×10^{15} molecules/cm^2. Over industrial complexes the corresponding range is 2.5 to 3.5×10^{15} molecules/cm^2 with indications for a seasonal variability with and amplitude of 4.0×10^{15} molecules/cm^2. Over rural areas the mean NO_2 tropospheric column densities range between 1.7 and 2.0×10^{15} molecules/cm^2. Over large cities the observed levels are lower than the ones observed over the most polluted areas of Southeast Asia and Central Europe which often exceed 11.0×10^{15} molecules/cm^2.

A twelve-month common dataset of GOME and SCIAMACHY shows a very good agreement (R=0.89) over the Balkan region. Long term common datasets of OMI and GOME-2 are also consistent with SCIAMACHY (R≈0.86). SCIAMACHY depicts higher NO_2 values than GOME due its finer horizontal resolution, whereas SCIAMACHY and GOME-2 show consistent values due to the similar overpass times and horizontal resolution. OMI observes lower NO_2 tropospheric columns than SCIAMACHY over mostly industrial and urban regions. This is mostly attributed to different local overpass times

ACPD
9, 12171–12205, 2009

of each satellite. The differences are affected by the local NO_2 diurnal variability due to a broad daily maximum in emission, combined with large photochemical loss of NO_2 around noon, which, however, can have different characteristics for each location. There is a relative decrease in the NO_2 column (around 3.03%) over the Balkan Peninsula deduced both by satellite measurements and CAMx predictions between 10:00 LT to 13:30 LT. However the ratio of the NO_2 tropospheric columns between 13:30 and 10:00 derived from OMI and SCIAMACHY is not constant a fact that is not reflected in the CAMx simulations. There is a consistent seasonality between the satellite and model determined ratios for the winter months (December–April) and there is a discrepancy in the seasonality during the summer months possibly due to the intense fire activity over the study area. Biomass burning emissions are not included in CAMx. Thus, there is an evident need for better understanding the 13:30/10:00 LT ratio differences between measurements and predictions.

NO_2 data from both GOME algorithms (TEMIS and Bremen) and CAMx predictions show moderate correlation (between 0.5 and 0.7), mostly because of missing CAMx biomass burning emissions and the absence of long range transport of pollution in the model estimates due to the clean boundary conditions chosen for the CAMx model (Katragkou et al., 2009). However the RMSE and MB estimates provide a consistent and slightly better result compared to previous studies, which indicates that for the purpose of air pollution management on a regional scale, highly resolved space-borne data are of great value. Particularly, UV/visible satellite measurements of tropospheric species provide valuable long-term data sets which can be used to evaluate current emission inventories used by various groups, to provide estimates for average conditions over areas with limited ground-based data availability and in addition they have a great potential to detect longterm trends in regional scale pollution.

Acknowledgements. CAMx simulations have been funded by the European Community's Sixth Framework Programme as part of the project CECILIA (Central and Eastern Europe Climate Change Impact and Vulnerability Assessment) under Contract No. 037005.

References

Acarreta, J. R., De Haan, J. F., and Stammes, P.: Cloud pressure retrieval using the O2-O2 absorption band at 477 nm, J. of Geophy. Res., 109, D05204, doi:10.1029/2003JD003915, 2004.

Bergman, J. W. and Salby, M. L.: Diurnal variations of cloud cover and their relationship to climatological conditions, J. Climate, 9, 2802–2820, 1996.

Blond, N., Boersma, K. F., and Eskes, H. J.: Intercomparison of SCIAMACHY nitrogen dioxide observations, in situ measurements and air quality modeling results over Western Europe, J. of Geophy. Res., 112, D10311, doi:10.1029/2006JD007277, 2007.

Boersma, K. F., Jacob, D. J., Trainic, M., Rudich, Y., DeSmedt, I., Dirksen, R., and Eskes, H. J.: Validation of urban NO2 concentrations and their diurnal and seasonal variations observed from space (SCIAMACHY and OMI sensors) using in situ measurements in Israeli cities, Atmos. Chem. Phys. Discuss., 9, 4301–4333, 2009, http://www.atmos-chem-phys-discuss.net/9/4301/2009/.

Boersma, K. F., Jacoba, D. J., Bucselab, E. J., Perringc, A. E., Dirksend, R., van der A, R. J., Yantoscaa, R. M., Parka, R. J., Wenigb, M. O., Bertramc, T. H., and Cohenc, R. C.: Validation of OMI tropospheric NO_2 observations during INTEX-B and application to constrain NO_x emissions over the eastern United States and Mexico, Atmos. Environment, 42, 4480–4497, 2008a.

Boersma, K. F., Jacob, D. J., and Eskes, H. J., et al.: Intercomparison of SCIAMACHY and OMI tropospheric NO_2 columns: observing the diurnal evolution of chemistry and emissions from space, J. Geophys. Res., 113, D16S26, doi:10.1029/2007JD008816, 2008b.

Boersma, K. F., Eskes, H. J., Veefkind, J. P., Brinksma, E. J., van der A, R. J., Sneep, M., van den Oord, G. H. J., Levelt, P. F., Stammes, P., Gleason, J. F., and Bucsela, E. J.: Near-real time retrieval of tropospheric NO2 from OMI, Atmos. Chem. Phys., 7, 2103–2118, 2007, http://www.atmos-chem-phys.net/7/2103/2007/.

Boersma, K. F., Eskes, H. J., and Brinksma, E. J.: Error analysis for tropospheric NO_2 retrieval from space, J. Geophys. Res., 109, D04311, doi:10.1029/2003JD003962, 2004.

Bovensmann, H., Burrows, J. P., Buchwitz, M., et al.: SCIAMACHY: Mission Objectives and Measurement Modes, J. Atmos. Sci., 56(2), 127–150, 1999.

Bradshaw, J., Davis, D., Grodzinsky, G., Smyth, S., Newell, R., Sandholm, S., and Liu, S.: Observed distributions of nitrogen oxides in the remote free troposphere from the NASA

global tropospheric experiment programs, Review of Geophysics, 38, 61–116, 2000.
Burrows, J. P., Weber, M., and Buchwitz, M., et al.: The global ozone monitoring experiment (GOME): Mission concept and first scientific results, J. Atmos. Sci., 151–157, 1999.
Callies, J., Corpaccioli, E., Eisinger, M., Hahne, A., and Lefebvre, A.: GOME-2- MetOp's Second Generation Sensor for Operational Ozone Monitoring, ESA Bulletin, No. 102, 2000.
Chipperfield, M. P.: Multiannual simulations with a threedimensional chemical transport model, J. Geophys. Res., 104, 1781–1805, 1999.
Crutzen, P. J.: The Role of NO and NO_2 in the Chemistry of the Troposphere and Stratosphere, Ann. Rev. Earth Pl. Sc., 7, 443–472 doi:10.1146/annurev.ea.07.050179.002303, 1979.
Dentener, F., van Weele, M., Krol, M., Houweling, S., and van Velthoven, P.: Trends and inter-annual variability of methane emissions derived from 1979–1993 global CTM simulations, Atmos. Chem. Phys., 3, 73–88, 2003, http://www.atmos-chem-phys.net/3/73/2003/.
Dickerson, R. R.: Measurements of reactive nitrogen compounds in the free troposphere, Atmos. Environment 18(12), 2585–2593, 1984.
Finlayson-Pitts, B. J., and Pitts Jr., J. N.: Chemistry of the Upper and Lower Atmosphere, J. Atmos. Chem., 39, 327–332, doi:0.1023/A:1010697311969, 2001.
He, Y., Uno, I., Wang, Z., et al.: Variations of the increasing trend of tropospheric NO_2 over central east China during the past decade, Atmos. Environ., 41, 4865–4876, 2007.
Heimann, M.: The global atmospheric tracer model TM2, Technical Report. 10, Deutsches Klimarechenzentrum, Hamburg, Germany, 1995.
Herman, J. R. and Celarier, E. A.: Earth surface reflectivity climatology at 340 m–380 m from TOMS data, J. Geophys. Res., 102(D23), 28003–28012, doi:10.1029/97JD02074, 1997.
Horowitz, L. W., Walters, S., Mauzerall, D. L., Emmons, L. K., Rasch, P. J., Granier, C., Tie, X., Lamarque, J. F., Schultz, M. G., Tyndall, G. S., Orlando, J. J., and Brasseur, G. P.: A global simulation of ozone and related tracers:description and evaluation of MOZART, Version 2, J. Geophys. Res., 108(D24), 4784, doi:10.1029/2002JD002853, 2003.
Koelemeijer, R. B. A., Stammes, P., Hovenier, J. W., and de Haan, J. F.: A fast method for retrieval of cloud parameters using oxygen A-band measurements from the Global Ozone Monitoring Instrument, J. Geophys. Res., 106, 3475–3490, 2001.
Koelemeijer, R. B. A., de Haan, J. F., and Stammes, P.: A database of spectral surface reflectivity in the range 335–772 nm derived from 5.5 years of GOME observations, J. Geophys. Res., 108(D2), 4070, doi:10.1029/2002JD002429, 2003.

Krüger, B. C., Katragkou, E., Tegoulias, I., Zanis, P., Melas, D., Coppola, E., Rauscher, S., Huszar, P., and Halenka, T.: Regional photochemical model calculations for Europe concerning ozone levels in a changing climate Quarterly Journal of the Hungarian Meteorological Service, 112(3–4), 285–300, July–December, 2008.

Kunhikrishnan, T., Lawrence, M. G., Kuhlmann, R., Richter, A., Ladstaatter-Weibenmayer, A., and Burrows, J. P.: Analysis of tropospheric NOx over Asia using the model of atmospheric transport and chemistry (MATCH-MPIC) and GOME satellite observations, Atmos. Environ., 38, 581–596, 2004.

Konovalov, I. B., Beekmann, M., Vautard, R., Burrows, J. P., Richter, A., Nüß, H., and Elansky, N.: Comparison and evaluation of modelled and GOME measurement derived tropospheric NO_2 columns over Western and Eastern Europe, Atmos. Chem. Phys., 5, 169–190, 2005, http://www.atmos-chem-phys.net/5/169/2005/.

Ladstätter-Weißenmayer, A., Kanakidou, M., and Meyer-Arnek, J.: Atmos. Environ., 41, 7262–7273, 2007.

Lambert, J. C., De Smedt, I., Granville, J., and Valks, P.: Initial validation of GOME-2 nitrogen dioxide columns (GDP 4.2 OTO/NO2 and NTO/NO2): March–June 2007, TN-IASB-GOME2-O3MSAF-NO2-01, Issue 1, Revision B, Technical Note/Validation Report, 2007.

Lee, D. S., Köhler, I., Grobler, E., Rohrer, F., Sausen, R., Gallardo-Klenner, L., Olivier, J. G. J., Dentener, F. J., and Bouwman, A. F.: Estimations of global NOx emissions and their uncertainties, Atmos. Environ., 31, 1735–1749, 1997.

Lefohn A. S.: Ozone, sulfur dioxide, and nitrogen dioxide trends at rural sites located in the United States, Atmos. Environ., 25A(2), 491–501, 1991.

Lelieveld, J., Berresheim, H., Borrmann, S., et al.: Global Air Pollution Crossroads over the Mediterranean, Science, 298(5594), 794, doi:10.1126/science.1075457, 2002.

Lelieveld, J. and Jansen, F. W.: Assessment of pollutant fluxes across the frontiers of the federal republic of Germany on the basis of aircraft measurements, Atmos. Environ., 23(5), 939–951, 1989.

Levelt, P. F., van der Ord, G. H. J., Dobber, M. R., et al.: The Ozone Monitoring Instrument, IEEE Trans. Geo. Rem. Sens. 44(5), 1093–1101, doi:10.1109/TGRS.2006.872333, 2006.

Mihalopoulos, N.: Long-Range transport of pollutants above the Eastern Mediterranean: Implications for air quality and regional climate, in: Regional climate variability and its impacts in the Mediterranean Area, editied by: Mellouki, A., and Ravishankara, A.R., Springer Netherlands, Netherlands, Volume 79, 1–13, 2007.

Onkal-Engin, G., Demir, I., and Hiz, H.: Assessment of urban air quality in Istanbul using fuzzy synthetic evaluation, Atmos. Environ., 38, 3809–3815, 2004.
Platt, U.: Differential Optical Absorption Spectroscopy (DOAS), in Air Monitoring by Spectroscopic Techniques, Chem. Anal., 127, edited by: Sigrist, M. W., 27–76, Wiley-Interscience, Hoboken, NJ, 1994.
Richter, A. and Burrows, J. P.: A multi wavelength approach for the retrieval of tropospheric NO_2 from GOME measurements, in proceedings of the ERS ENVISAT symposium, Gothenburg, October, 2000.
Richter, A. and Burrows, J. P.: Tropospheric NO_2 for GOME measurements, Adv. Space Res., 29(11), 1673–1683, 2002.
Richter, A., Burrows, J. P., Nüß, H., et al.: Increase in tropospheric nitrogen dioxide over China observed from space, Nature, 437, 129–132, doi:10.1038/nature04092, 2005.
Schaub, D., Boersma, K. F., Kaiser, J. W., Weiss, A. K., Folini, D., Eskes, H. J., and Buchmann, B.: Comparison of GOME tropospheric NO_2 columns with NO_2 profiles deduced from ground-based in situ measurements, Atmos. Chem. Phys., 6, 3211–3229, 2006, http://www.atmos-chem-phys.net/6/3211/2006/.
Seinfeld, J. H. and Pandis, S. N.: Atmospheric Chemistry and Physics: From Air Pollution to Climate Change, J. Wiley, New York, 1998.
Shettle, E. P. and Fenn, R. W.: Models of the atmospheric aerosols and their opticalproperties, in AGARD Conference Proceedings No. 183, ADA028–615, 1976.
Solomon, S., Portmann, R., Sandres, W., et al.: On the role of nitrogen dioxide in the absorption of solar radiation, J. Geophys. Res., 104(D10), 12047–12058, 1999.
van der A, R.J., Eskes, H.J., van Roozendael, M., De Smedt, I., Blond, N., Boersma, F., Weiss, A.: TEMIS Algorithm Document Tropospheric NO2, KNMI, Netherlands, 21pp, available at: http://www.temis.nl/docs/AD_NO2.pdf, 2006.
Uno, I., He, Y., Ohara, T., Yamaji, K., Kurokawa, J.-I., Katayama, M., Wang, Z., Noguchi, K., Hayashida, S., Richter, A., and Burrows, J. P.: Systematic analysis of interannual and seasonal variations of model-simulated tropospheric NO_2 in Asia and comparison with GOME-satellite data, Atmos. Chem. Phys., 7, 1671–1681, 2007, http://www.atmos-chem-phys.net/7/1671/2007/.
Van der A, R. J., Eskes, H. J., Boersma, K. F., et al.: Trends, seasonal variability and dominant NO_x source derived from a ten year record of NO_2 measured from space, J. Geophys. Res., 113, D04302, doi:10.1029/2007JD009021, 2008.

Van der A, R. J., Peters, D. H. M. U., Eskes, H., Boersma, K. F., Van Roozendael, M., De Smedt, I., and Kelder, H. M.: Detection of the trend and seasonal variation intropospheric NO_2 over China, J. Geophy. Res., 111, D12317, doi:10.1029/2005JD006594, 2006.

van Noije, T. P. C., Eskes, H. J., Dentener, F. J., Stevenson, D. S., Ellingsen, K., Schultz, M. G., Wild, O., Amann, M., Atherton, C. S., Bergmann, D. J., Bey, I., Boersma, K. F., Butler, T., Cofala, J., Drevet, J., Fiore, A. M., Gauss, M., Hauglustaine, D. A., Horowitz, L. W., Isaksen, I. S. A., Krol, M. C., Lamarque, J.-F., Lawrence, M. G., Martin, R. V., Montanaro, V., Müller, J.-F., Pitari, G., Prather, M. J., Pyle, J. A., Richter, A., Rodriguez, J. M., Savage, N. H., Strahan, S. E., Sudo, K., Szopa, S., and van Roozendael, M.: Multi-model ensemble simulations of tropospheric NO2 compared with GOME retrievals for the year 2000, Atmos. Chem. Phys., 6, 2943–2979, 2006, http://www.atmos-chem-phys.net/6/2943/2006/.

Table 1. Sources and characteristics of satellite tropospheric NO_2 data used in this study.

Instrument	Satellite platform	Start date	End date	Equator crosstime	Horizontal resolution
GOME (KNMI/BIRA) [Version 1.04]	ERS-2	03/1996	06/2003	10:30 LT	320×40 km^2
GOME (IUP BREMEN) [Version 2.0]	ERS-2	01/1996	06/2003	10:30 LT	320×40 km^2
SCIAMACHY (KNMI/BIRA) [Version 1.10]	ENVISAT	07/2002	10/2008	10:00 LT	60×30 km^2
OMI (KNMI/BIRA) [Version 1.0.2 collection 3]	EOS AURA	10/2004	10/2008	13:30 LT	13×24 km^2
GOME-2 (KNMI/BIRA) [Version 1.1]	METOP	04/2007	10/2008	09:30 LT	80×40 km^2

ACPD
9, 12171–12205, 2009

Table 2. Mean values and standard deviations of tropospheric NO_2 columns in 10^{15} molecules/cm^2 estimated from GOME, SCIAMACHY, OMI and GOME-2 for the urban (U), rural (R) and industrial (I) geolocations considered in this study.

Metropolis	Label	Latitude	Longitude	GOME		SCIA		OMIT3		GOME-2	
				Mean	σ	Mean	σ	Mean	σ	Mean	σ
Beligrade	U	44.798	20.466	3.5	2.7	4.5	3.7	4.8	3.6	4.2	3.0
Bucharest	U	44.436	26.127	3.0	1.6	3.4	2.4	3.7	3.0	3.5	2.4
Sarajevo	U	43.850	18.419	1.9	1.1	2.1	2.0	1.9	1.4	1.8	1.8
Sofia	U	42.679	23.320	2.5	1.6	2.9	2.3	2.8	2.4	2.7	2.9
Pristina	U	42.655	21.181	1.8	1.5	2.1	1.5	2.1	1.5	1.8	1.3
Podgorica	U	42.434	19.281	1.5	1.0	1.5	1.4	1.4	1.0	1.5	1.4
Skopje	U	42.001	21.453	2.1	1.4	2.8	2.4	2.5	1.9	2.2	1.8
Prilep	U	41.351	21.562	3.2	2.1	2.9	2.9	2.5	2.1	2.4	2.1
Tirana	U	41.322	9.849	1.4	0.9	1.6	1.4	1.8	1.2	1.6	1.1
Xanthi	U	41.137	24.893	2.1	1.6	1.9	1.5	2.1	1.5	1.6	1.6
Constantinople	U	41.065	29.005	6.0	4.5	8.2	6.8	6.5	6.1	7.1	6.0
Thessaloniki	U	40.622	22.971	4.7	3.1	4.7	4.1	4.2	3.8	3.9	3.8
Athens	U	39.989	23.773	3.4	2.0	5.0	4.2	4.0	3.4	4.5	3.1
Ioannina	U	39.655	20.852	2.4	1.4	1.6	1.2	1.8	1.3	1.6	1.3
Izmir	U	38.425	27.142	3.3	1.8	4.6	3.0	3.2	1.9	4.1	2.4
Antalya	U	36.892	30.709	1.5	0.9	1.7	1.1	1.6	1.0	1.8	1.1
Heraklio	U	35.265	25.141	1.2	0.6	1.1	0.7	1.3	0.8	1.2	0.7
Nikosia	U	35.165	33.348	1.4	0.8	1.5	1.4	1.6	1.2	1.6	1.1
Athos	R	42.305	24.161	2.9	2.2	1.9	1.8	1.7	1.3	1.8	1.7
Othonoi	R	39.838	18.403	1.6	1.1	1.4	1.0	1.4	1.0	1.7	1.2
Agios Efstratios	R	39.516	24.999	1.9	1.0	1.7	1.3	1.5	1.1	1.8	1.2
Thessaly	R	39.499	22.633	3.2	2.1	4.2	3.4	3.2	2.6	2.9	2.5
Aliartos	R	38.379	23.110	3.3	1.9	2.6	2.4	2.8	2.2	2.8	2.5
Zakynthos	R	37.797	20.754	1.3	0.7	1.2	0.8	1.4	1.0	1.4	1.0
Strofades	R	37.246	21.005	1.3	0.8	1.2	0.7	1.3	0.9	1.3	1.2
Kythira	R	36.261	23.081	1.3	0.7	1.4	0.9	1.4	1.0	1.5	1.0
Rhodes	R	36.166	28.000	1.5	0.9	1.6	1.0	1.4	1.0	1.8	1.1
Finokalia	R	35.338	25.667	1.2	0.6	1.0	0.6	1.2	0.7	1.2	0.7
Kozlodui	I	43.780	24.205	2.4	1.5	2.6	1.6	2.8	1.8	2.9	2.0
Maritsa	I	42.155	24.426	2.6	1.2	2.7	2.0	3.2	2.3	2.6	1.7
Ptolemaida	I	40.521	21.696	4.0	2.4	5.9	5.8	4.5	4.4	4.1	3.4
Megalopoli	I	37.402	19.281	1.9	1.0	1.6	1.0	1.8	1.2	1.5	1.0

ACPD
9, 12171–12205, 2009

Table 3. The statistical values of the comparison between GOME and CAMx tropospheric NO_2 monthly averages. The unit is 10^{15} molecules/cm^2.

		Industrial	Rural	Urban	CHIMERE vs. SCIAMACHY (TEMIS algorithm document)
GOMEtemis	RMSE	1.50	0.88	1.88	2.9
	MB	−0.11	0.07	−0.21	0.2
GOMEbremen	RMSE	1.45	1.25	1.75	–
	MB	0.63	−0.40	−0.03	–

Fig. 1. Spatial distribution of the geolocations considered.

ACPD
9, 12171–12205, 2009

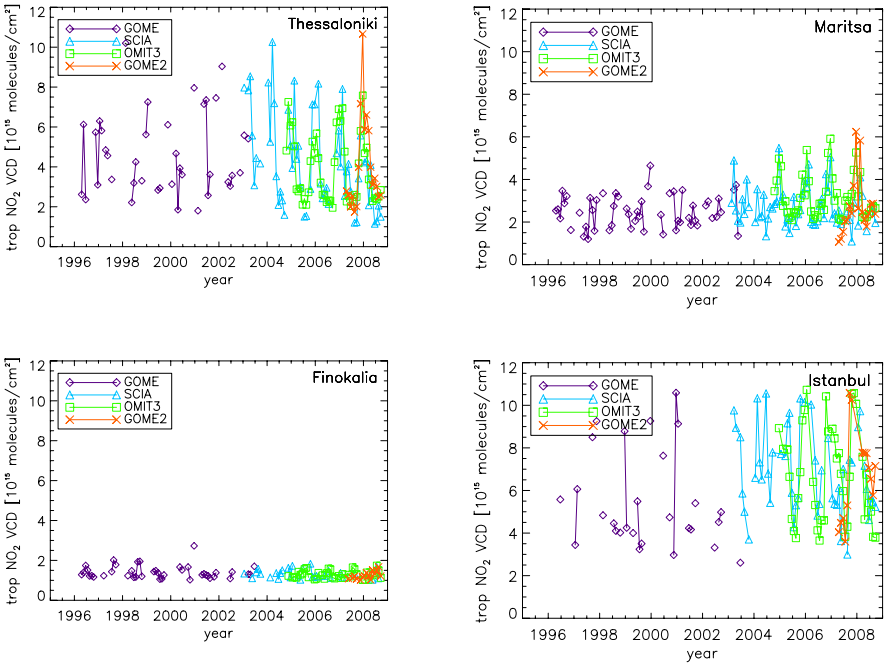

Fig. 2. Time series analysis of satellite-measured NO_2 tropospheric columns for Thessaloniki (upper left), Maritsa (upper right), Finokalia (lower left) and Istanbul (lower right).

ACPD
9, 12171–12205, 2009

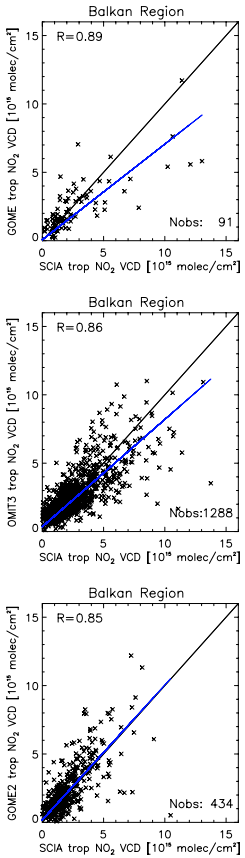

Fig. 3. Scatter plots of GOME (upper), OMI (middle) and GOME-2 (bottom) versus SCIAMACHY tropospheric NO_2 columns (in 10^{15} molecules/cm^2) for the entire region. Each point represents a monthly mean value for each geolocation. Nobs are the number of data. The solid line indicates y=x.

ACPD
9, 12171–12205, 2009

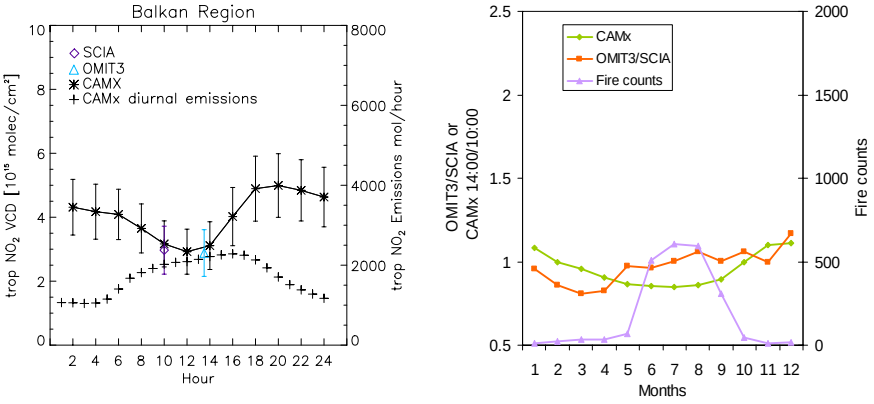

Fig. 4. Left panel: Average diurnal variation of tropospheric NO_2 columns modeled (from 1996 to 2001) by CAMx (asterisk symbols) and observed by SCIAMACHY (from 2004 to 2008) at 10:00LT (diamonds symbol) and OMI (from 2004 to 2008) at 13:30 LT (triangle symbol) for the Balkan geolocations. The crosses indicate the average diurnal variation of CAMx NO_2 emissions over a 50×50 km grid of the area under study. Right panel: Concurrent monthly average ratios of tropospheric NO_2 satellite measurements (OMIT3 over SCIAMACHY), model simulations (CAMx 14:00/10:00) over urban areas and the total monthly fire counts over the Balkan geolocations for the time period 2004–2008.

ACPD
9, 12171–12205, 2009

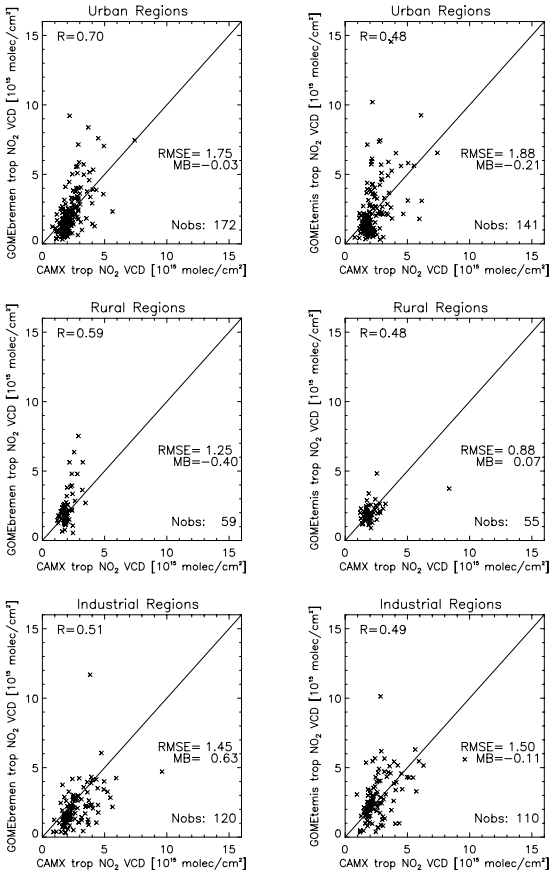

Fig. 5. Scatter plots of GOMEbremen (left plots) and GOMEtemis (right plots) monthly NO_2 tropospheric columns (y axis) versus NO_2 CAMx tropospheric columns (x axis) for urban (top), rural (middle) and industrial (bottom) regions. Columns are in 10^{15} molecules/cm^2. *R* is the correlation coefficient. Nobs is the number of observations. The solid line represents the y=x

ACPD
9, 12171–12205, 2009

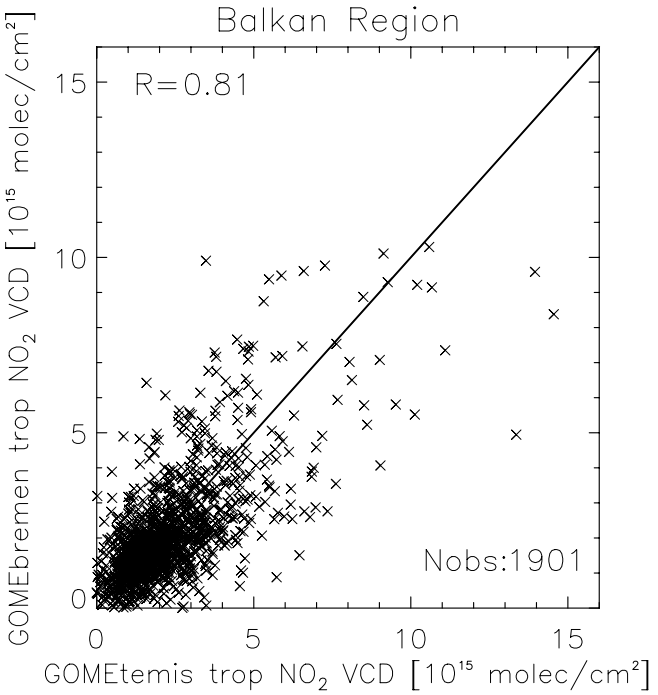

Fig. 6. Scatter plot of GOMEbremen versus GOMEtemis tropospheric NO_2 columns for all Balkan geolocations. Nobs is the number of observations.

ACPD
9, 12171–12205, 2009

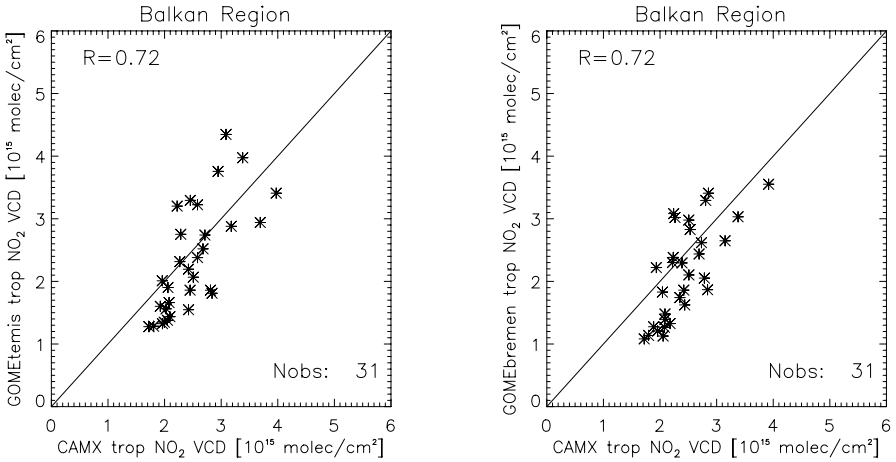

Fig. 7. Tropospheric NO_2 VCDs (10^{15} molecules/cm^2) from GOMEtemis (left) and GOMEbremen (right) versus NO_2 model tropospheric predictions at the ensemble of 31 geolocations. Each diamond symbol corresponds to the average tropospheric NO_2 column, derived from concurrent daily values for the time period 1996–2001, over a geolocation. *R* is the correlation coefficient. Nobs is the number of observations.

ACPD
9, 12171–12205, 2009